The Bioscan
AN INTERNATIONAL QUARTERLY JOURNAL OF LIFE SCIENCES
20(2): 34-39, 2025 www.thebioscan.com

Design, pharmacophore based screening, docking and molecular simulation study of some novel pyrazine derivatives against Mycobacterium tuberculosis Fatty Acid Synthase I

AKHILESH KUMAR BILAIYA[1*], DR GAJANAND ENGLA[2]

1,2 School of Pharmacy, Devi Ahilya University, Indore

akhileshbilaiya@gmail.com

DOI: 10.63001/tbs.2025.v20.i02.pp34-39

KEYWORDS
Pyrazine,
Pharmacophore,
Mycobacterium tuberculosis Fatty Acid Synthase I,
Docking,
Molecular simulation

Received on:

01-03-2025

Accepted on:

07-04-2025

Published on

12-05-2025

ABSTRACT

This manuscript elucidates the conceptualization and computational assessment of innovative pyrazine derivatives. A pharmacophore-based screening approach was done toward the identification of lead compounds based on a developed pharmacophore model encapsulating critical structural features for the inhibition of FAS. 274 pyrazine derivative of seven series S1, S2, S3, S4, S5, S4, and S7 were designed and screened for drug likeness. 273 passed drug likeness filter were screened using high-throughput virtual screening to filter candidates with an optimal pharmacophore fit score. Molecular docking studies were then carried out on 16 selected compounds (S1-20, S1-31, S2-14, S2-18, S3-22, S4-21, S6-21, S6-13, S6-18, S6-24, S6-25, S6-28, S7-19, S7-2, S7-17, and S7-26) against the active site of Mycobacterium tuberculosis Fatty Acid Synthase I (FAS I) . Molecular dynamics simulations were then performed with the S6-25. An integrated computational approach here identified S6-25 having good potential as inhibitors of FAS I.

INTRODUCTION

Mycobacterium tuberculosis (Mtb) is the infectious illness that causes tuberculosis (TB), which continues to be a leading cause of death worldwide although up to 25% of people worldwide exhibit signs of exposure to Mtb. Only a tiny percentage go on to acquire symptomatic tuberculosis, which translates to about 13.6 million new instances and 1.3 million mortalities globally in 2022.[1] Mtb that is resistant to two powerful isoniazid and rifampin, is the cause of multidrug-resistant TB (MDR-TB). 10.6 million Individuals had tuberculosis in 2022, and 410,000 new cases (about 3.3%) of MDR and rifampicin-resistant TB were detected while strains resistant to rifampin monotherapy or MDR-TB account for 17% of cases of TB that have already received treatment.[1] Since the COVID-19 pandemic, the frequency of MDR-TB cases has been rising. This trend has been made worse by ongoing wars in several nations that impede prompt and efficient medical care. [2] Historically, drug-resistant tuberculosis treatment regimens have been hazardous, costly, and time-consuming—up to 18 to 24 months. This lowers the quality of life of the patients and causes major medical and financial obligations.[3] Patient's life quality, course of the treatment, and medication adherence may all be enhanced by the development of time frame treatment for rifampin-resistant TB and MDR-TB [4]. The organism that causes tuberculosis (TB), Mycobacterium tuberculosis (Mtb), is known to be a strong foe. Drugs find it difficult to get through its thick, waxy cell wall and reach the targeted molecular target (s). Furthermore, Mtb has a variety of drug-resistant mechanisms, including efflux pumps. [5]

Pyrazine and its analogues have attracted a lot of interest as possible building blocks for hybrid molecules due to their varied pharmacological characteristics.[6] In the treatment of TB, pyrazinamide is the main pharmacotherapeutic agent and is frequently used with other anti-TB drugs. Its strong anti-TB effectiveness is essential for reducing the length of tuberculosis treatment.[7] Numerous pyrazinamide modifications have been investigated as potent antitubercular medications. Bioisosteric alterations of the derivatives that have pyrazinamide ring, leading to the creation of strong antitubercular drug.[8,9] Pyrazolopyridones represent a novel class of decaprenylphosphoryl-ß-D-ribose-2'-epierase inhibitors exhibiting significant anti-mycobacterial efficacy. [10] Zhou and his research team have identified the antitubercular properties of carboxamide substitutes pyrazine. [11] Kumar et al. have documented a series of pyrazine derivatives that show promise as inhibitors of decaprenylphosphoryl-ß-D-ribose-2'-epierase for the therapeutic management of tuberculosis.[12] Pyrazines exhibits particular structure–activity relationships (SAR) in terms of anti-TB capabilities. When pyrazine derivatives were outfitted with electron-withdrawing groups, their activity increased. [13] The development of novel scaffolds as possible antitubercular medicines is of great interest due to the high toxicity, high load, and prolonged therapy of conventional treatments, as well as the emergence of drug resistance. [14] Therefore, in order to get around the current drug resistance problem, further work is required to create and synthesize novel anti-TB drugs that have distinct mechanisms of action in order to increase the number of treatment options available. This study intends to demonstrate

the design of a variety of new substituted molecules by changing the pyrazine ring in order to evaluate the compounds' ability to fight tuberculosis, analyze their interactions using virtual screening based on Pharmacophore modelling and docking.

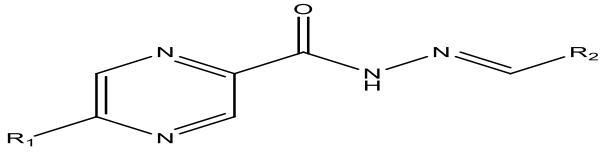

Figure 1: General structure of designed Pyrazine derivatives

Three-dimensional crystal structure of Mycobacterium TB Fatty Acid Synthase I (PDBID: 6GJC) with a resolution of 3 Å was selected and downloaded from Protein Data Bank (https://www.rcsb.org) one the basis of co-crystallized with a ligand, and excellent resolution.[16]

2.3 Generation of Pharmacophore Model

To create reliable structure-based pharmacophore models, Biovia Discovery Studio (DS) 4.1 (Biovia Dassault Systems, Discovery Studio 2021) were used.

2.4 Virtual screening

2.4.1 The Lipinski and Veber filters

The Lipinski and Veber filters were used to assess the drug likeness of every designed compound.

2.4.2 Pharmacophre based virtual screenig

Designed library was virtually screened using the produced pharmacophore models as parameters. The BEST conformation approach produced 59479 conformers out of 273 drug like molecule. Each hit's fit values and related molecular descriptor after being identified by QSAR predictions 16 compounds were then the focus of a docking investigation.

2.4.3 Molecular docking study

2.4.3.1 Protein preparation

Using the DS, macromolecular and nonmolecular components were separated while hydrogen polar was added to the receptor to prepare it.

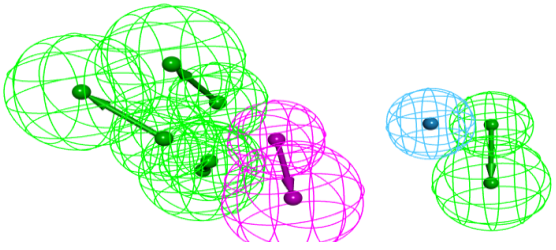

Figure 2: Generated Pharmacophore model wherein Green: hydrogen bond acceptor, Violet: hydrogen bond donor, and Sky Blue: Hydrophobic features.

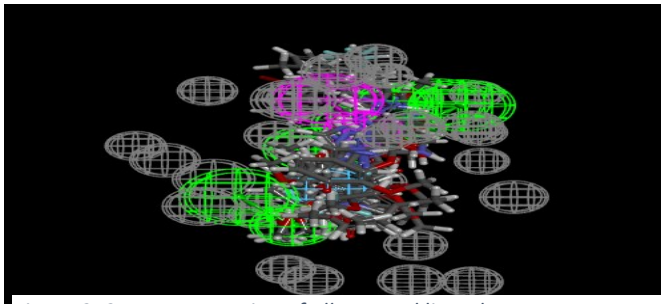

Figure 3: 3D representation of all mapped ligand

Inhibitor of Mycobacterium TB Fatty Acid Synthase-I, 5-chloropyrazinoic acid (5Cl-PZA), were docked into the active site of Mycobacterium tuberculosis Fatty Acid Synthase-I protein. Docking scores were a key factor in choosing the optimal positions for the docked compounds, and molecules were ordered based on these scores. The docking data and binding pattern of all 16 molecules were analyzed, and it was discovered that they were more active than 5Cl-PZA at the binding site in the protein

2. Material and Method

2.1 Designing of Pyrazine derivatives

A library of 274 Pyrazine derivatives (figure 1) of seven series S1, S2, S3, S4, S5, S4, and S7 with various functional groups was created in order to investigate a variety of physicochemical characteristics. As a result, the library was designed and draw their 2D structure using Chem Draw Ultra 12.0 and saved mol format , compatible with Discovery Studio to include analogues with various substituted phenoxy, methoxy, and chloro groups at the R1 and various substituted aromatics at the R2.[15]

2.2 Selection of target protein

2.4.3.2 Ligand preparation

The energy minimization of all ligands was performed using ligand preparation tool in small molecule wizard in DS.

2.4.3.3 Molecular docking analysis

DS were used to perform docking study and to find out molecular interactions. The primary objective of the docking analysis was to critically assess the binding affinity between the ligand and the receptor. The ligand-receptor binding affinity was estimated using the Libdock score.

2.4.4 ADMET analysis

The pharmacokinetic and toxicological attributes were evaluated utilizing ADMET analysis, which concurrently facilitated the prediction of physicochemical properties such as hydrogen bond donors/acceptors, molecular polar surface area (TPSA), molecular weight and the quantity of rotatable bonds (NRB)], in addition to pharmacokinetics [blood–brain barrier (BBB) permeability, Gastrointestinal absorption (GIA), , P-glycoprotein (P-gp) substrate interaction, and cytochrome P450 (CYP) enzyme inhibition].

2.4.5 Molecular dynamics (MD) simulations

Molecular dynamics (MD) simulations ligands and the complexes of the target protein were performed using iMODS: Internal coordinate's normal mode analysis server [17], iMod: Internal Coordinates NMA [18] and Deformability [19].

3. Results and Discussion

3.1 Pharmacophore modelling

Ten distinct pharmacophore models were generated utilizing the receptor based pharmacophore generation methodology provided by DS. The predominant characteristics of the pharmacophore models consist of hydrophobic interactions (Hbic), hydrogen bond acceptors (HBA) and hydrogen bond donors (HBD).

3.2 Virtual screening

As previously indicated, a comprehensive data set comprising 273 compounds, curated based on existing literature, was employed utilizing the BEST search methodology to ascertain the potential hit molecules, and the Pharmacophore model featuring a minimum of six characteristics as depicated in Figure 2 (one hydrophobic feature, four hydrogen bond acceptors and one hydrogen bond donor) was chosen for the purpose of virtual screening. 21 poses of 16 compounds out of all virtually screened compounds found to align with the Pharmacophore model. The fit value of best poses of 16 compounds ranges 3.09569-0.616678 shown in table 2.

3.3 Molecular docking

The six chains that make up the Mycobacterium tuberculosis Fatty Acid Synthase-I protein (PDB ID 6GJC) are A, B, C, D, E, and F. Chain A represents the whole protein, while chains B, C, D, E, and F indicate the attached DNA. Except for chain A, every chain was taken out. The co-crystallized ligand flavin mononucleotide (FMN) served as the basis for defining the active site. Using a protein preparation module, protein was created after heteroatoms were removed and polar hydrogen was added. By re-docking FMN, the molecular modeling approach was validated (Figure 4).

Mycobacterium TB Fatty Acid Synthase-I. Table 3 listed both the docking score.

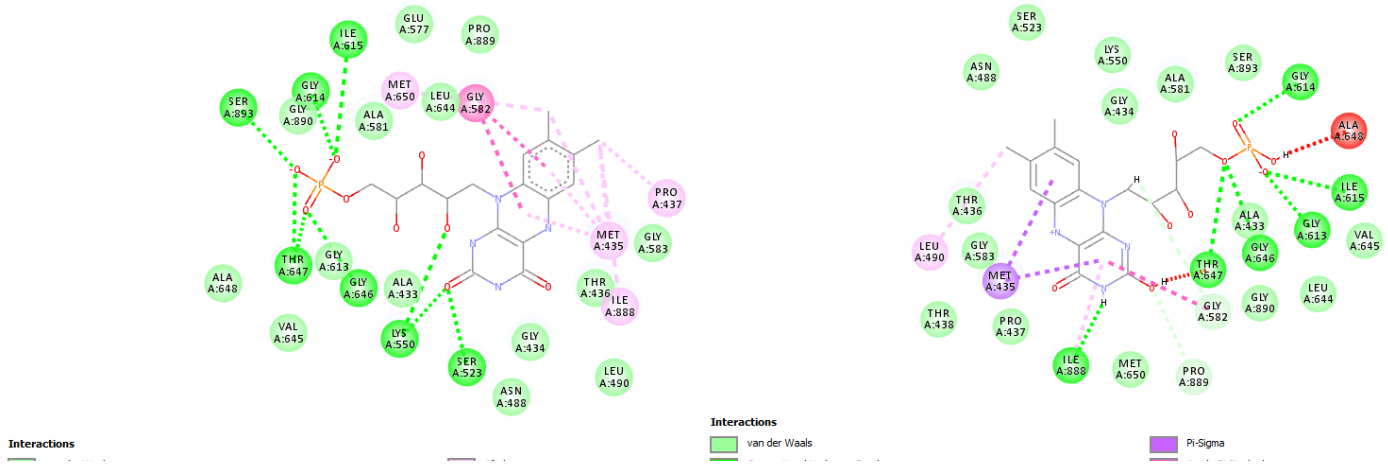

Figure 4: 2D representation of interaction of flavin mononucleotide (FMN) and Mycobacterium tuberculosis Fatty Acid Synthase - I, Left- Pre-dock Right Re-dock.

Table 1: docking score of 5Cl-PZA and all 16 molecules, Fit values of best poses of 16 compounds align with the Pharmacophore model and ADMET and Toxicity Prediction

S. No.	Name	Lib Dock Score	Best fit	Solubility Lavel	BBB Lavel	CYP2D6 Prediction	ADMET Absorption Lavel	PPB Lavel	TOPKAT Ames Prediction
1	S6-25	126.369	1.26927	2	3	FALSE	0	TRUE	Non-Mutagen
2	S2-18	122.571	1.44198	2	4	FALSE	0	TRUE	Non-Mutagen
3	S7-26	118.165	2.51091	3	3	FALSE	0	TRUE	Non-Mutagen
4	S1-20	118.072	2.21905	2	3	FALSE	0	TRUE	Non-Mutagen
5	S7-19	117.715	2.08837	3	3	FALSE	0	TRUE	Non-Mutagen
6	S1-31	116.597	2.72201	3	3	FALSE	0	TRUE	Non-Mutagen
7	S6-18	115.281	2.09633	2	4	TRUE	0	TRUE	Non-Mutagen
8	S6-13	114.95	0.61667	2	4	FALSE	1	TRUE	Non-Mutagen
9	S7-17	111.801	2.61455	3	3	FALSE	0	TRUE	Non-Mutagen
10	S7-2	111.217	2.83194	3	2	FALSE	0	TRUE	Non-Mutagen
11	S2-14	107.817	2.09627	2	4	FALSE	1	TRUE	Non-Mutagen
12	S6-21	107.517	2.58208	2	4	TRUE	0	TRUE	Non-Mutagen
13	S6-28	107.451	3.09569	2	3	FALSE	0	TRUE	Non-Mutagen
14	S6-24	105.542	2.51919	2	4	TRUE	1	TRUE	Non-Mutagen
15	S3-22	104.991	1.49157	1	4	FALSE	1	TRUE	Non-Mutagen
16	S4-21	97.1032	2.53521	2	4	FALSE	0	TRUE	Non-Mutagen
17	5-Cl-PZA	68.6339							

The 5Cl-PZA's docking score was 68.6339. As seen in Figure 5A, 5Cl-PZA was able to generate three π donor hydrogen bonds with GLY646, THR647, and GLY890, the optimal molecule S625 exhibited the two hydrogen bonds with isoleucine 615 and serine 893, in addition to two carbon-hydrogen bonds with alanine 581 and leucine 644. Furthermore, a hydrogen bond was noted with the isoleucine 615; additionally, a carbon-hydrogen bond was identified with isoleucine 888, a halogen bond with glycine 434, a π donor hydrogen bond with glycine 646, a pi-sigma bond with threonine 436, an amide-π stacking interaction with glycine 582, and four alkyl interactions with methionine 435, leucine 490, valine 645, and alanine 648, correlating with a docking score of 126.369 as illustrated in Figure 6. A total of sixteen potential compounds were successfully derived through the synergistic application of drug design tools. These compounds underwent subsequent evaluations utilizing ADMET and toxicity predictions, culminating in molecular dynamics simulation investigations.

3.4 ADMET and Toxicity Prediction

The cessation of principal molecules through clinical investigations is frequently attributed to suboptimal pharmacokinetic characteristics and concerns regarding toxicity. Therefore, it would be advantageous from an economic perspective if these problems had been identified early on. Given this, it would be prudent to use the in-silico methodology to forecast the potential toxicity and pharmacokinetic properties of the hit compounds in order to identify lead molecules. [20,21]. Toxicity and ADMET results are enlisted in Table 3.

Compounds S131, S72, S717, S719, and S726 having solubility lavel 3 predicts good aqueous solubility at 25°C [22]. All the Compounds having BBB Lavel 2-4, higher value BBB Lavel predicts

lower brain/blood concentration ratio after oral administration. CYP2D6 predictive classification (False = Non-inhibitor, True = Inhibitor) [23]. The PPB level (True) serves as an indicator for the binding affinity to blood plasma proteins [24]. Ames mutagenicity assays were conducted on all sixteen identified potential candidates. The assessment of toxicity risk for the compounds indicated that all sixteen compounds are classified as Non-Mutagenic.

3.5 Molecular Dynamics Simulation

To evaluate the stability and physical movements of the docked complexes iMOD server was employed. The dynamics were scrutinized, revealing significant amplitude conformational variations through the application of normal mode analysis (NMA). B-factor and deformability metrics elucidated the mobility of S625-6GJC complexes. S625-6GJC complexes' B-factor and deformability metrics exhibit peaks that link with the sections of the protein that display significant deformability; the most prominent peaks signify areas with discriminating deformability. A comparative analysis of the normal mode analysis (NMA) and PDB fields for the complexes is illustrated by the B-factor graphs (Figures 7). Each normal mode exhibits an inverse correlation with both variance and eigenvalue. Figures 8 and 9 present the graphs corresponding to the eigenvalue and variance of the S625-6GJC complexe, respectively. Purple-shaded bars on the target proteins' variation graph indicate individual variance, whereas green-shaded bars show cumulative variance. The covariance matrix for the S625-6GJC complexes illustrates the inter-residue correlations within the complex. In this matrix, the quality of the complex is positively correlated with the degree of correlation observed the uncorrelated motion, substantial correlation and anti correlation between residues indicated by white, red and blue coloration respectively as shown in figure 10. Figure 11 elucidate the elastic maps which represent the relationships among the atoms. The darker gray areas indicate the stiffer regions of the S625-6GJC complexes.

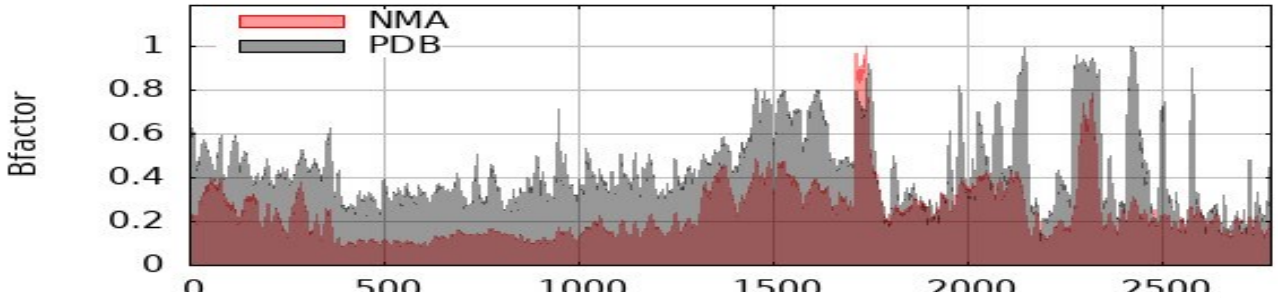

Figure 7: A comparison of the complexes' NMA and PDB fields is shown by the B-factor graphs

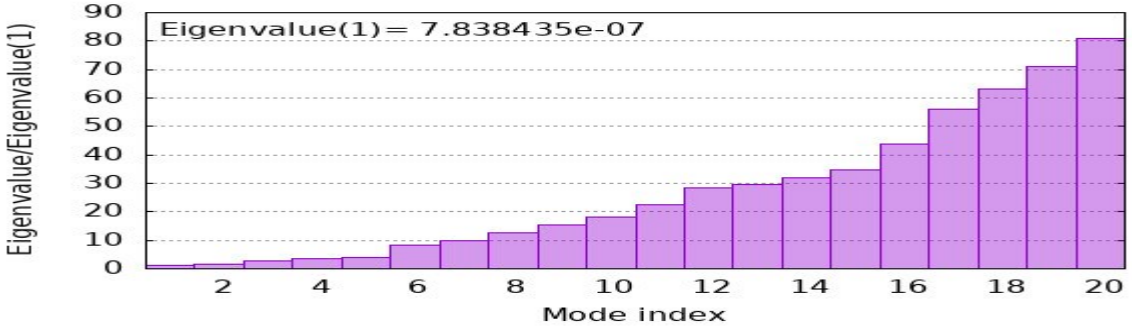

Figure 8: eigenvalue graph

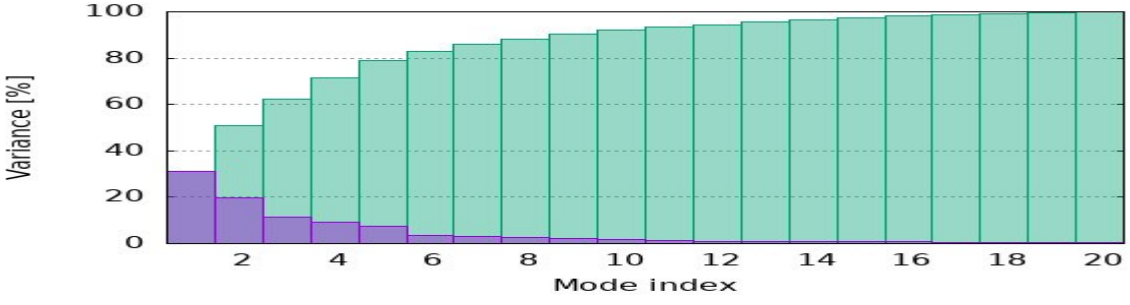

Figure 9: variance graph

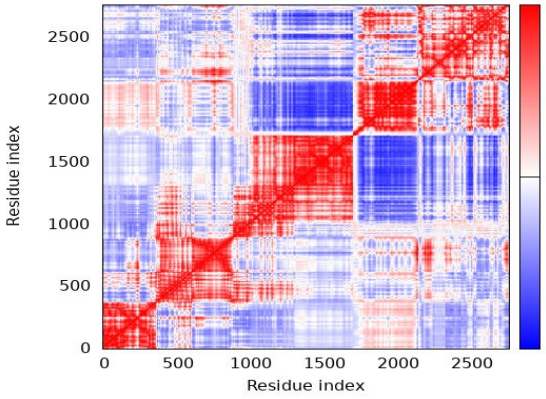

Figure 10: covariance matrix of the S625-6GJC complex

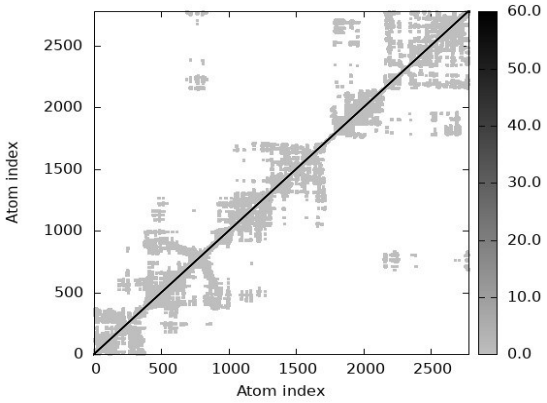

Figure 11: elastic maps of the S625-6GJC complex

DISCUSSION

The study concluded with the creation of a structure-based pharmacophore model for the protein Fatty Acid Synthase-I in Mycobacterium TB. Hypo1 was chosen from ten other Hypothesis of generated pharmacophores. A virtual screening of 274 designed compounds using selected pharmacophore model gave 16 hits. The LibDock methodology on DS docked 16 hits—which were obtained by imposing different constraints—on the active sites of the Mycobacterium TB Fatty Acid Synthase-I protein (PDB ID: 6GJC). The standard 5Cl-PZA ligand was used to compare all 16 hit compounds, their docking scores, and their interactions with the active site residues. Under the TOPKAT initiative, all 16 compounds underwent toxicity evaluation and ADMET investigations. S6-25 was chosen for additional MD simulation based on the findings of the ADMET, toxicity assessment and docking. Compound S6-25 was determined to be stable based on all the experiments, and it can be used to build possible novel inhibitors of Mycobacterium tuberculosis Fatty Acid Synthase-I.

Acknowledgment

Author would like to acknowledge Sri Aurobindo Institute of Pharmacy, Indore for providing CADD Lab facility to perform the computational studies.

REFERENCES

- WHO. Global tuberculosis report 2023. https://www.who.int/teams/ global-tuberculosis-programme/tb-reports/global-tuberculosisreport-2023 (accessed Jan 28, 2024).
- Saluzzo, F., & Cirillo, D. M. (2023). Mind the gap. Rolling out new drug resistant tuberculosis regimens with limited diagnostic tools. *Journal of Clinical Tuberculosis and Other Mycobacterial Diseases*, *32*.
- Falzon, D., Jaramillo, E., Schünemann, H. J., Arentz, M., Bauer, M., Bayona, J., & Zignol, M. (2011). WHO guidelines for the programmatic management of drug-resistant tuberculosis: 2011 update.
- Krishna, S., & Jacob, J. J. (2021). Diabetes mellitus and tuberculosis.
- Singh, V. (2024). Tuberculosis treatment-shortening. *Drug Discovery Today*, 103955.
- B. Miniyar, P., R. Murumkar, P., S. Patil, P., A. Barmade, M., & G. Bothara, K. (2013). Unequivocal role of pyrazine ring in medicinally important compounds: a review. *Mini reviews in medicinal chemistry*, *13*(11), 1607-1625.
- Zhang, Y., Shi, W., Zhang, W., & Mitchison, D. (2014). *Mechanisms of pyrazinamide action and resistance. Microbiol Spectr 2: MGM2-0023-2013.*
- Reddyrajula, R., & Dalimba, U. (2020). The bioisosteric modification of pyrazinamide derivatives led to potent antitubercular agents: Synthesis via click approach and molecular docking of pyrazine-1, 2, 3-triazoles. *Bioorganic & Medicinal Chemistry Letters*, *30*(2), 126846.
- Reddyrajula, R., & Dalimba, U. (2020). The bioisosteric modification of pyrazinamide derivatives led to potent antitubercular agents: Synthesis via click approach and molecular docking of pyrazine-1, 2, 3-triazoles. *Bioorganic & Medicinal Chemistry Letters*, *30*(2), 126846.
- Panda, M., Ramachandran, S., Ramachandran, V., Shirude, P. S., Humnabadkar, V., Nagalapur, K., Raichurkar, A. (2014). Discovery of pyrazolopyridones as a novel class of noncovalent DprE1 inhibitor with potent anti-mycobacterial activity. *Journal of medicinal chemistry*, *57*(11), 4761-4771.
- Zhou, S., Yang, S., & Huang, G. (2017). Design, synthesis and biological activity of pyrazinamide derivatives for anti-Mycobacterium tuberculosis. *Journal of Enzyme Inhibition and Medicinal Chemistry*, *32*(1), 1183-1186.
- Dinesha, P., Udayakumar, D., Shetty, V. P., & Deekshit, V. K. (2024). Design, synthesis, characterization, and biological evaluation of novel pyrazine-1, 3, 4-oxadiazole/[1, 2, 4] triazolo [3, 4-b][1, 3, 4] thiadiazine hybrids as potent antimycobacterial agents. *Journal of Molecular Structure*, *1304*, 137657.
- Naik, S., Puttachari, D., Vanishree, A. L., Udayakumar, D., Shetty, V. P., Prabhu, C., & Deekshit, V. K. (2024). Synthesis and biological evaluation of novel hybrid compounds bearing pyrazine and 1, 2, 4-triazole analogues as potent antitubercular agents. *RSC Pharmaceutics*.
- Orenstein, E. W., Basu, S., Shah, N. S., Andrews, J. R., Friedland, G. H., Moll, A. P., ... & Galvani, A. P. (2009). Treatment outcomes among patients with multidrug-resistant tuberculosis: systematic review and meta-analysis. *The Lancet infectious diseases*, *9*(3), 153-161.
- Abdel-Aziz, M., & Abdel-Rahman, H. M. (2010). Synthesis and anti-mycobacterial evaluation of some pyrazine-2-carboxylic acid hydrazide derivatives. *European journal of medicinal chemistry*, *45*(8), 3384-3388.
- Al-Najjar BO, Abbas MA, Sibai OA, Saqallah FG, Al-Kabariti AY (2023) QSAR, structure- based pharmacophore modelling and biological evaluation of

novel platelet ADP receptor (P2Y 12) antagonist. RSC Medicinal Chemistry 14: 239–246.

- López-Blanco, J. R., Aliaga, J. I., Quintana-Ortí, E. S., & Chacón, P. (2014). iMODS: internal coordinates normal mode analysis server. *Nucleic acids research*, *42*(W1), W271-W276.
- Lopéz-Blanco, J. R., Garzón, J. I., & Chacón, P. (2011). iMod: multipurpose normal mode analysis in internal coordinates. *Bioinformatics*, *27*(20), 2843-2850.
- Kovacs, J. A., Chacón, P., & Abagyan, R. (2004). Predictions of protein flexibility: first-order measures. *Proteins: Structure, Function, and Bioinformatics*, *56*(4), 661-668.
- Ponnan, P., Gupta, S., Chopra, M., Tandon, R., Baghel, A. S., Gupta, G., & Raj, H. G. (2013). 2D-QSAR, Docking Studies, and In Silico ADMET Prediction of Polyphenolic Acetates as Substrates for Protein Acetyltransferase Function of Glutamine Synthetase of Mycobacterium tuberculosis. *International Scholarly Research Notices*, *2013*(1), 373516.
- Gaur, R., Cheema, H. S., Kumar, Y., Singh, S. P., Yadav, D. K., Darokar, M. P., & Bhakuni, R. S. (2015). In vitro antimalarial activity and molecular modeling studies of novel artemisinin derivatives. *RSC advances*, *5*(59), 47959-47974.
- Cheng, A., & Merz, K. M. (2003). Prediction of aqueous solubility of a diverse set of compounds using quantitative structure− property relationships. *Journal of medicinal chemistry*, *46*(17), 3572-3580.
- Susnow, R. G., & Dixon, S. L. (2003). Use of robust classification techniques for the prediction of human cytochrome P450 2D6 inhibition. *Journal of chemical information and computer sciences*, *43*(4), 1308-1315.
- Dixon, S. L., & Merz, K. M. (2001). One-dimensional molecular representations and similarity calculations: methodology and validation. *Journal of Medicinal Chemistry*, *44*(23), 3795-3809.